HHS Public Access

Author manuscript

Cell Rep. Author manuscript; available in PMC 2018 January 02.

Published in final edited form as:

Cell Rep. 2017 December 05; 21(10): 2785–2795. doi:10.1016/j.celrep.2017.11.020.

Differential effects of EGFL6 on tumor *versus* wound angiogenesis

Kyunghee Noh[1,4,†], **Lingegowda S. Mangala**[1,3,†], **Hee-Dong Han**[5,†], **Ningyan Zhang**[6], **Sunila Pradeep**[1,7], **Sherry Y. Wu**[1], **Shaolin Ma**[1], **Edna Mora**[8], **Rajesha Rupaimoole**[1], **Dahai Jiang**[1,3], **Yunfei Wen**[1], **Mian MK Shahzad**[1], **Yasmin Lyons**[1], **MinSoon Cho**[9], **Wei Hu**[1], **Archana S. Nagaraja**[1], **Monika Haemmerle**[1], **Celia SL Mak**[1], **Xiuhui Chen**[1], **Kshipra M. Gharpure**[1], **Hui Deng**[6], **Wei Xiong**[6], **Charles V Kingsley**[10], **Jinsong Liu**[11], **Nicholas Jennings**[1], **Michael J. Birrer**[12], **Richard R. Bouchard**[10], **Gabriel Lopez-Berestein**[2,3,13], **Zhiqiang An**[6], and **Anil K. Sood**[1,2,3,14,*]

[1]Department of Gynecologic Oncology and Reproductive Medicine, The University of Texas MD Anderson Cancer Center, Houston, Texas 77030, USA

[2]Department of Cancer Biology, The University of Texas MD Anderson Cancer Center, Houston, Texas 77030, USA

[3]Center for RNA Interference and Non-Coding RNA, The University of Texas MD Anderson Cancer Center, Houston, Texas 77030, USA

[4]Gene Therapy Research Unit, Korea Research Institute of Bioscience and Biotechnology, Daejeon, Republic of Korea

[5]Department of Immunology, School of Medicine, Konkuk University, Chungju, 380-701, South Korea

[6]Texas Therapeutics Institute, Brown Foundation Institute of Molecular Medicine, The University of Texas Health Science Center at Houston, Houston, Texas 77030, USA

[7]Department of Obstetrics and Gynecology, Medical College of Wisconsin, Milwaukee, WI, 53226, USA

[8]Department of Surgery, University of Puerto Rico, San Juan 00936, Puerto Rico; University of Puerto Rico Comprehensive Cancer Center, San Juan 00936, Puerto Rico; Department of Surgical Oncology, The University of Texas MD Anderson Cancer Center, Houston, Texas 77584, USA

[*]Correspondence and requests for materials should be addressed to asood@mdanderson.org.

[14]**Lead Contact:** Anil K. Sood, asood@mdadnerson.org, Tel)713-745-5266, FAX)713-792-7586

[†]Kyunghee Noh, Lingegowda S. Mangala and Hee-Dong Han contributed equally to this work.

AUTHOR CONTRIBUTIONS

A.K.S. and H.H. designed the project. K.N., L.M., N.Z. and S.P. designed the experiments. K.N., L.M., E.M., S.M., R.R and M.M.S performed the experimental work. J.L., M.J.B., R.R.B. and G.L analyzed the results. Z.A., W.X., H.D. and C.V.K. contributed reagents and expertise. K.N., L.M., S.P. and A.K.S wrote the manuscript with input from all co-authors.

Conflicts of interest: The authors declare no conflicts of interest related to this work.

[9]Department of Benign Hematology, The University of Texas MD Anderson Cancer Center, Houston, Texas 77030, USA

[10]Department of Imaging Physics, The University of Texas MD Anderson Cancer Center, Houston, TX 77030

[11]Department of Pathology, The University of Texas MD Anderson Cancer Center, Houston, TX 77030

[12]Massachusetts General Hospital, Boston, MA02114

[13]Department of Experimental Therapeutics, The University of Texas MD Anderson Cancer Center, Houston, TX 77030

SUMMARY

Angiogenesis inhibitors are important for cancer therapy, but clinically approved anti-angiogenic agents have shown only modest efficacy and can compromise wound healing. This necessitates development of novel anti-angiogenesis therapies. Here, we show significantly increased EGFL6 expression in tumor- *versus* wound or normal endothelial cells. Using a series of *in vitro* and *in vivo* studies with orthotopic and genetically engineered mouse models, we demonstrate the mechanisms by which EGFL6 stimulates tumor angiogenesis. In contrast to its antagonistic effects on tumor angiogenesis, EGFL6 blockage did not affect normal wound healing. These findings have significant implications for development of anti-angiogenesis therapies.

Graphical Abstract

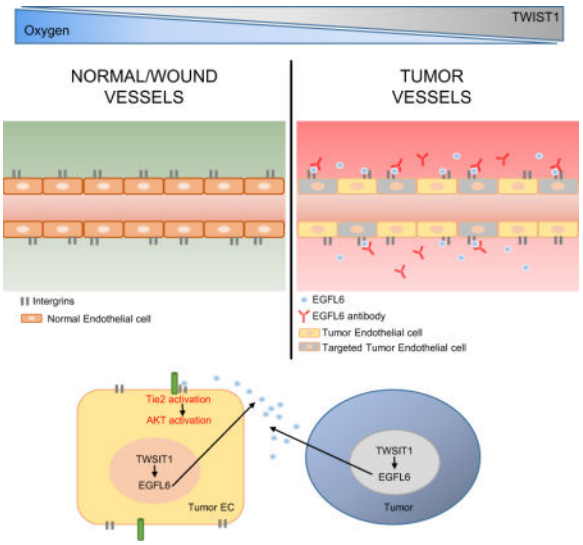

Keywords

Tumor endothelial cells; ovarian cancer; chitosan nanoparticles; tumor vasculature; wound healing

INTRODUCTION

Angiogenesis is essential for many physiological and pathological processes such as embryogenesis, pregnancy, wound healing, tumor growth, and metastasis (Bergers and Benjamin, 2003, Breier, 2000, Tonnesen et al., 2000, Eming et al., 2007, Gressett and Shah, 2009, Shord et al., 2009). To date, multiple anti-angiogenesis drugs (e.g., bevacizumab) have been developed and tested. While modest efficacy has been noted with this class of drugs against many cancers, specific adverse effects such as hypertension and impaired wound healing have been a significant concern (Gressett and Shah, 2009, Shord et al., 2009, Koskas et al., 2010). Therefore, we asked whether targets unique for tumor angiogenesis could be identified and used for therapeutic development. To address this question, we carried out a series of experiments to identify targets that are differentially expressed in tumor angiogenesis. Among these, EGFL6 (EGF like domain multiple 6) was found to be highly expressed in tumor-associated endothelial cells compared to normal ovarian and wound-associated endothelial cells. EGFL6, also called MAEG, is a secreted protein that belongs to the epidermal growth factor (EGF) repeat superfamily. EGFL6 was mapped to the human Xp22 chromosome and has been shown to be expressed during early development, mainly in fetal tissues of lung, skin, umbilical cord, liver/spleen, and placenta but not in normal adult tissues (Yeung et al., 1999, Buchner et al., 2000). While it has been shown to be expressed in some tumors (Wang et al., 2012, Buckanovich et al., 2007), its unique role in tumor angiogenesis identifies it as an important target that does not impair wound healing.

RESULTS

EGFL6 is upregulated in tumor-associated endothelial cells

To identify candidate targets that are important for tumor angiogenesis, but not wound healing, we first isolated endothelial cells from 10 high-grade serous ovarian cancers (HGSC), 5 normal ovarian tissues, and 7 healing wound patient samples. RNA was isolated and subjected to genomic analyses. We found that 375 genes were upregulated in HGSC endothelial cells compared with those from normal ovarian and healing wound tissues (Fig. 1a). Among these genes, *EGFL6* showed the highest differential expression (52.63-fold higher) in tumor endothelial cells compared with normal ovarian endothelial cells (Fig. 1b). Expression of EGFL6 and VEGF in ovarian patient samples was examined. As expected, VEGF was expressed in ovarian cancer tissues and in healing wounds (Supplementary Fig. 1a), but EGFL6 was expressed mainly in tumor associated endothelial cells (Fig. 1c). To further validate the microarray results, we isolated endothelial cells from an independent cohort of normal ovarian, HGSC, and wound tissues and examined *EGFL6* expression using qRT-PCR. *EGFL6* was predominantly expressed in tumor endothelial cells, but not in normal ovary or wound endothelial cells (Fig. 1d).

Next, we studied the biological implications of EGFL6 upregulation in tumor endothelial cells. To investigate the biological functions of EGFL6 in tumor angiogenesis, RF24 cells were treated with *EGFL6* siRNA. There was more than 80% knockdown in EGFL6 protein levels within 72 hours compared with non-targeting siRNA in control cells (Supplementary Fig. 1b). *EGFL6* siRNA-treated cells showed significantly reduced tube formation and migration compared to control siRNA-treated cells (Supplementary Fig. 1c, d).

EGFL6 silencing did not affect wound healing in mice

Since EGFL6 expression was not increased in wound endothelial cells, we next asked whether *EGFL6* silencing would have any effect on wound healing. To address this question, we used a wound healing mouse model. As expected, treatment with DC101 (VEGFR2-blocking antibody) (Witte et al., 1998, Zhu et al., 1998) resulted in significant impairment of wound healing (Fig. 2a and Supplementary Fig. 2a). To test the potential effects of EGFL6 on tumor growth and wound healing, we examined *EGFL6* mRNA levels in ovarian cancer cells (Supplementary Fig. 2b). We used our well-characterized chitosan (CH) nanoparticle delivery system that is highly efficient for delivery to tumor vasculature (Lu et al., 2010, Masiero et al., 2013, Krzeszinski et al., 2014) (Supplementary Fig. 2c). Mouse *EGFL6* siRNA (m*EGFL6* siRNA)-CH had no significant effect on wound healing compared with control siRNA-CH (Fig. 2b and Supplementary Fig. 2d). However, mouse *EGFL6* siRNA–CH treated animals had significant reduction in SKOV3ip1 ovarian tumor burden (Fig. 2c–e). *EGFL6* gene silencing resulted in significant reduction in proliferation indices and tumor microvessel density (Supplementary Fig. 2e). As shown in Supplementary Figure 2f and g, treatment of SKOV3ip1 tumor-bearing animals with mouse *EGFL6* siRNA alone and with a combination of mouse and human *EGFL6* siRNA resulted in significant reduction in tumor growth compared to controls. However, treatment with human *EGFL6* siRNA alone did not affect tumor growth, indicating that EGFL6 from endothelial cells is more decisive for tumor growth and angiogenesis (Supplementary Fig. 2h). A major difference between tumor and wound is the extent of hypoxia (Peng et al., 2012, Carmeliet and Jain, 2000, Schafer and Werner, 2008). Given the differences in EGFL6 expression between tumor and wound endothelial cells, we asked whether hypoxia could be an important factor in regulating EGFL6 levels. To address this question, we created hind limb ischemia on mice by ligating the femoral artery on the hind limb of the mouse (Fig. 2f) (Krishna et al., 2016). As shown in Figure 2g, ischemic tissues showed significant increase in EGFL6 levels in endothelial cells. Blood flow was recovered by 96 hours after ligation of femoral artery.

TWIST1 enhances EGFL6 for hypoxia-triggered angiogenesis

To identify potential mechanisms of EGFL6 regulation in the tumor microenvironment, we next investigated EGFL6 transcriptional activity. Under hypoxia, EGFL6 promoter activity was significantly increased compared with levels under normoxia (Fig. 3a). Upon promoter analysis, Twist1 transcription factor was predicted to bind to the EGFL6 promoter (Supplementary Fig. 3a). Of interest, EGFL6 transcriptional activity levels were similarly increased with ectopic expression of TWIST1, further supporting a link between TWIST1 and EGFL6 (Fig. 3b). Treatment of cells with $CoCl_2$, a HIF1-α stabilizer, also resulted in increased *EGFL6* and *TWIST1* levels (Fig. 3c).

Next, we ectopically expressed *TWIST1* in RF24 endothelial cells and measured *EGFL6* levels. We found a significant increase in *EGFL6* levels in endothelial cells with elevated *TWIST1* compared with control cells (Fig. 3d). Moreover, we silenced *TWIST1* with siRNA, and *EGFL6* levels did not increase under hypoxia conditions following *TWIST1* silencing (Supplementary Fig. 3b). Upon ChIP analysis with anti-TWIST1 antibody, the binding of TWIST1 to the *EGFL6* promoter region was significantly higher under hypoxic *versus* normoxic conditions (Fig. 3e). Since EGFL6 expression was enhanced under hypoxic

conditions, we next asked whether increased EGFL6 levels contribute to survival of endothelial cells under hypoxic conditions. To address this question, we silenced *EGFL6* in RF24 cells under hypoxia by using *EGFL6* siRNA and determined the percentage of cell death. As shown in Figure 3f, almost 50% of cells survived the hypoxic conditions, even after 5 days, compared with those under normoxic conditions. In contrast, *EGFL6* gene silencing under hypoxia resulted in > 75% cell death.

EGFL6-mediated Tie2/PI3K/AKT signaling

To further understand the signaling events downstream of EGFL6, we conducted reverse phase protein array (RPPA) analyses of EGFL6-treated RF24 endothelial cells and untreated control cells. EGFL6-treated endothelial cells showed activation of PI3K/AKT signaling (Supplementary Fig. 4a and Fig. 4a). To further validate these results, we treated RF24 endothelial cells with EGFL6 and examined for AKT and PI3K signaling (Fig. 4b and Supplementary Fig. 4b). EGFL6-treated RF24 cells showed increased expression of p-PI3K and p-AKT compared with untreated cells. The migration (Supplementary Fig. 4c) and tube formation (Supplementary Fig. 4d) of RF24 cells increased significantly after treatment with EGFL6, and these EGFL6-induced functions were completely blocked in the presence of a PI3K inhibitor, suggesting the key involvement of PI3K signaling. To identify candidate proteins involved in EGFL6-mediated AKT activation, we used a phospho-RTK array and found activation of 3 RTKs, including IGF-1R, EGFR, and Tie2 (Supplementary Fig. 4e). We confirmed these results in EGFL6-treated RF24 cells using Western blot analysis. As shown in Figure 4c, only Tie2 was activated in EGFL6-treated cells. EGFL6 contains RGD motifs that can bind to integrins (Chim et al., 2011).

To gain insight into the mechanisms through which EGFL6 promotes Tie2 and αVβ3 or α5β1 binding capacity, we examined which integrins could bind to the Tie2 receptor. The potential interaction between α5β1 integrin and the Tie2 receptor was confirmed by co-immunoprecipitation in the presence of EGFL6 (Fig. 4d). Tie2 is broadly expressed on the membrane in cells. After stimulation with EGFL6, we tested whether it could be activated in the cell membrane. We determined Tie2 and AKT activation levels in the cytosolic and membrane fractions. Activation of Tie2 was substantially enhanced in EGFL6-stimulated cell membrane fractions (Fig. 4e).

We next examined the effect of silencing *integrins* and *Tie2* on EGFL6-induced angiogenesis in RF24 cells. Silencing *β1* integrin or *Tie2* by using specific siRNA resulted in 80–90% reduction of expression (Fig. 4f). As shown in Figures 4g and h, silencing of *β1* integrin or *Tie2* significantly reduced both tube formation and migration. The addition of EGFL6 after silencing of these two components did not rescue either of these functions. We also determined the interaction of EGFL6 with integrins by using a RGD blocking peptide and evaluated its effects on EGFL6-mediated functions. As shown in Figures 4i–k, endothelial cells treated with RGD blocking peptide showed significant reduction in tube formation and migration compared with EGFL6-treated cells. Collectively, these data indicate that EGFL6 regulates Tie2/AKT signaling through α5β1 integrin to promote endothelial cell migration and tube formation. However, *EGFL6* silencing in the SKOV3ip1 cancer cells did not affect

Tie2/AKT signaling (Supplementary Fig. 4f). Similarly, EGFL6-treated RMG2 tumor cells did not show significant changes in PI3K/AKT signaling (Supplementary Fig. 4g).

EGFL6 antibody blocks tumor angiogenesis

Given the robust anti-angiogenesis effects with silencing EGFL6, we next aimed to develop neutralizing antibodies and tested their effects on angiogenesis. To identify monoclonal antibodies (mAbs) targeting EGFL6, we screened a large panel of monoclonal antibodies (>3000) produced from single memory B cells isolated from PBMCs of a rabbit immunized with human EGFL6 and more than 300 clones showed high EGFL6 binding by ELISA (Supplementary Fig. 5a–b). Two functional mAbs (mAb #93 and mAb #135) were characterized further (Supplementary Fig. 5a and 5c) and used for both *in vitro* and *in vivo* experiments. Figure 5a shows concentration dependence of high affinity binding on human EGFL6 by the two lead mAbs. Kinetic binding constants (Kd) of the two mAbs to human EGFL6 were 1.89 nM for mAb#93 and 2.19 nM for mAb #135 (Supplementary Fig. 5d).

As shown in Figure 5b, treatment of endothelial cells with EGFL6 blocking antibodies #93 and #135 resulted in reduction in expression of both phosphorylated Tie2 and AKT (Supplementary Fig. 5e). We also examined potential effects of these antibodies on wound-healing. EGFL6 neutralizing antibody had no effect on wound healing *in vivo* (Fig. 5c). EGFL6-mediated functional effects on tube formation (Fig. 5d) and migration (Fig. 5e) were completely blocked by EGFL6-targeted antibodies.

Next, we determined whether anti-EGFL6 antibodies could block tumor angiogenesis *in vivo*. Human ovarian cancer (SKOV3ip1) or breast cancer (MDA-MB-231) tumor-bearing mice (n=10 mice per group) were treated with either control or anti-EGFL6 antibodies. After 5 weeks of treatment, tumors were harvested and checked for anti-tumor and anti-angiogenic effects. Anti-EGFL6 antibodies displayed potent anti-tumor activity compared to control antibody. Treatment with either anti-EGFL6 antibody #93 or #135 resulted in significant reduction in tumor growth (Fig. 5f and Supplementary Fig. 5f). Tumors treated with the EGFL6 targeted antibody showed decreased cell proliferation and MVD compared with those from the control antibody-treated groups (Fig. 5g and Supplementary Fig. 5g).

EGFL6 silencing inhibits tumor growth and angiogenesis

To further determine the role of EGFL6 during tumor development, conditional EGFL6$^{fl/fl}$ mice were generated and crossed with *Tie2-Cre* transgenic mice, thereby targeting cre recombinase in endothelial cells (Supplementary Fig. 6a). We isolated endothelial cells from *wild-type* (*WT*) and *Tie2;EGFL6* knockout (*KO*) mice (Supplementary Fig. 6b). As shown in Supplementary Figure 6c, *EGFL6* mRNA was not expressed in *EGFL6* knockout endothelial cells. There was no significant difference observed either in weight or the morphology of organs such as lung, liver, kidney, spleen and heart in *WT* and *KO* mice (Supplementary Fig. 6 d, e). For testing the role of EGFL6 expression under ischemic conditions, we created hind limb ischemia on *WT* and *KO* mice by ligation of the femoral artery in hind limb of mice (Supplementary Fig. 6f). Blood flow was recovered by 96 hours after ligation of femoral artery in both *WT* and *KO* mice. To identify the role of EGFL6 in tumor endothelial cells, we injected *WT* and *KO* mice with murine ID8 ovarian cancer or

murine E0771 breast cancer cells. We detected EGFL6 expression in the tumor vasculature in *WT* mice, but not in *KO* mice (Fig. 6b). We compared the tumor burden in *WT* and *KO* mice and found that tumor weight in *KO* mice was significantly lower compared to that of *WT* mice (Fig. 6a and c, Supplementary Fig. 6g). Furthermore, tumor cell proliferation and MVD were lower in tumor-bearing *KO* mice than in tumor-bearing *WT* mice (Fig. 6d, e).

To evaluate potential clinical relevance of EGFL6, we examined 130 high-grade serous ovarian cancers. Increased vascular expression of EGFL6 was noted in 73% of the samples (Fig. 6f). Increased expression of EGFL6 in tumor vasculature was significantly associated with high-stage ($p<0.002$; Supplementary Table 1) disease and was related to poor overall survival ($p<0.001$; Fig. 6g).

DISCUSSION

Our findings identify major differences in tumor compared to wound angiogenesis. Among these, EGFL6 was found to be increased in tumor endothelial cells in response to hypoxia mediated TWIST1 and AKT pathway activation (Supplementary Fig. 6h). On the basis of these data, we generated EGFL6-targeted monoclonal antibodies that bind effectively to EGFL6 with high-affinity and block tumor angiogenesis without impacting wound healing.

VEGF has been recognized as a key target for anti-angiogenesis therapy. However, current angiogenesis inhibitors can cause intolerable adverse effects, including bleeding and impaired wound healing. Currently, the most broadly used anti-angiogenesis drug is bevacizumab, a monoclonal antibody that blocks the activity of VEGF-A (Ferrara and Kerbel, 2005). Given the effects of anti-VEGF drugs on wound healing, they cannot be safely used perioperatively. Therefore, identifying targets that have differential expression between normal and tumor angiogenesis could be highly valuable for improving the efficacy and safety of anti-angiogenesis approaches. The observed effects of EGFL6-blocking monoclonal antibodies in impairing tumor angiogenesis and growth without impacting wound healing indicate this to be such a target.

EGFL6 is a member of the EGF domain containing EGF repeat superfamily of proteins. It is known to be expressed in some tissues such as benign meningioma, mouse microvascular endothelial cells, and ovarian and oral squamous cell carcinomas (Bai et al., 2016, Chim et al., 2011, Chuang et al., 2017, Oberauer et al., 2010, Buckanovich et al., 2007). It is also known to be expressed in some fetal tissues (Yeung et al., 1999). In a recent report, EGFL6 was found to be a stem cell regulatory factor in ovarian cancer and regulates ALDH+ ovarian cancer stem-like cells *via* SHP2/ERK signaling pathway. Moreover, vascular EGFL6 expression was found to mediate ovarian tumor growth (Bai et al., 2016). While several signaling pathways are potentially activated in various tissues by EGFL6, we provide an understanding of EGFL6 function in triggering integrin/Tie2/AKT signaling, which is a potent angiogenesis regulating signaling axis. EGFL6 levels in tumor endothelial cells were found to be regulated by TWIST1.

EGFL7, another EGF–like family protein, is also highly expressed in vasculature (Schmidt et al., 2007). It has been reported that delayed development of vasculature in organs was

found in EGFL7 knock-out mice due to inhibition of angiogenesis by blocking autocrine Notch signaling in vasculature (Nichol and Stuhlmann, 2012). Moreover, the MMRRC has reported that female EGFL6 KO mice (deleted exon-1) are embryonic lethal. However, mechanisms underlying expression of EGFL6 in various tissues and embryonic lethality are not fully understood. Here, we generated endothelial cell specific knock-out mice with Tie2-cre mice, which was not associated with lethality in both female and male mice. Also, all organs tested were morphologically normal. Although many angiogenic factor knock-out mice are embryonic lethal, the EGFL6;Tie2 knock-out mice are viable and could be a powerful tool for biological studies. In summary, we have demonstrated that EGFL6 levels are selectively increased in tumor endothelial cells and represent an attractive therapeutic target for inhibiting ovarian and other cancers while mitigating off-target effects and toxicity.

MATRIALS AND METHODS

Cell lines and culture

Human Breast Cancer cell line MDA-MB-231 and human epithelial ovarian cancer cell lines SKOV3ip1, HeyA8, A2274, A2780, OVCAR5, OVCAR8, RMG2, and IGROV1 were maintained as described previously (Pradeep et al., 2015). Human immortalized umbilical endothelial cells (RF24) and human dermal microvascular endothelial cells were grown in MEM medium with supplements (sodium pyruvate, non-essential amino acids, MEM vitamins, and glutamine; Life Technologies, Grand Island, NY). The derivation and characterization of the mouse ovarian endothelial cells has been described previously (Langley et al., 2003). Cell cultures were maintained at 37°C in a 5% CO_2 incubator with 95% humidity. For *in vivo* injections, cells were trypsinized and centrifuged at 1,200 rpm for 5 min at 4°C, washed twice with PBS, and reconstituted in serum-free Hank's balanced salt solution (Life Technologies). Only single-cell suspensions with more than 95% viability (as determined by trypan blue exclusion) were used for *in vivo* injections.

Endothelial cell isolation

Fresh tissue samples (5 normal ovaries, 7 wound tissues, and 10 epithelial high-grade, stage III or IV invasive serous ovarian cancers) were obtained from patients undergoing primary surgical exploration after approval from the Institutional Review Board. Total RNA from purified endothelial cells was subjected to microarray analysis by using the Affymetrix Human U133 plus 2.0 GeneChip platform (Lu et al., 2007).

Quantitative real-time reverse-transcriptase PCR validation

Quantitative real-time reverse-transcriptase RT-PCR was performed by using 50 ng of total RNA from purified endothelial cells, which were isolated by using the RNeasy mini kit (Qiagen) according to the manufacturer's instructions. Complementary DNA (cDNA) was synthesized from 0.5–1 μg of total RNA by using a Verso cDNA kit (Thermo Scientific). Quantitative PCR (qPCR) analysis was performed in triplicate by using the appropriate primers (Supplementary table 2) and the SYBR Green ER qPCR SuperMix Universal (Invitrogen, Carlsbad, CA) and Bio-Rad (Bio-Rad Laboratories, Hercules, CA). Relative quantification was calculated by using the $2^{-\Delta\Delta CT}$ method normalizing to control for percent fold changes (Donninger et al., 2004).

SiRNA constructs and delivery

SiRNAs were purchased from Sigma-Aldrich (Woodlands, TX). A non-silencing siRNA that did not share sequence homology with any known human mRNA based on a BLAST search was used as the control for target siRNA. *In vitro* transient transfection was performed as described previously (Landen et al., 2005). Briefly, siRNA (4 μg) was incubated with 10 μL of Lipofectamine 2000 transfection reagent (Lipofectamine) for 20 min at room temperature according to the manufacturer's instructions and added to cells in culture at 80% confluence in 10 cm culture plates.

RPPA and Western blot analysis

RF24 and RMG2 cells in the presence or absence of human recombinant EGFL6 protein were subjected to RPPA analysis. Western blot analysis was performed as previously reported (Pradeep et al., 2015, Haemmerle et al., 2017). Cell lysate of RF24 cells were treated with human recombinant EGFL6 protein or anti-EGFL6 antibodies and checked for activation of PI3kinase and AKT signaling by using anti-human EGFL6, PI3kinase, and AKT antibodies followed by secondary antibodies conjugated with horseradish peroxidase. Experiments were done in duplicate and performed three times.

Phosphorylated RTK array

A human phosphorylated RTK array kit (R&D Systems) was used to detect the relative tyrosine phosphorylation level of 42 different RTKs, in RF24 cells treated with human recombinant EGFL6 protein for 15 min. The human EGFL6 recombinant protein was obtained from Sinobiological (Beijing, China).

Cell migration assay

Using Transwell poer Polycarbonate Membrane inserts coated with 0.1% gelatin, we assessed the migration of the RF24 cells in the presence or absence of h*EGFL6* siRNA. After post-transfection of 48 h with h*EGFL6*, *integrin*, or *Tie2* siRNAs or after post-transfection of 6 h with EGFL6 antibody, PI3kinase inhibitor, or GRGDSP, RF24 cells (1.0×10^5) in MEM serum-free medium were seeded into the upper chamber of the Transwell 0.4 μm pore Polycarbonate Membrane insert (Corning, Lowell, MA). The insert was placed in a 24-well plate containing MEM medium with 15% serum in the lower chamber as chemoattractant. Cells were allowed to migrate in a humidified incubator for 6 h. Cells that had migrated were stained with use of hematoxylin and were counted by light microscopy in five random fields (×200 original magnification) per sample. Experiments were done in duplicate and performed three times.

Tube formation assay

Matrigel (12.5 mg/mL) was thawed at 4°C, and 50 μL was quickly added to each well of a 96-well plate and allowed to solidify for 10 min at 37°C. The wells were then incubated for 6 h at 37°C with RF24 cells (5,000 per well), which had previously been treated with *EGFL6*, *integrin beta 1*, or *Tie2* siRNA (for 48 h) or EGFL6 antibody, PI3kinase inhibitor, or GRGDSP (for 6 h). Experiments were performed in triplicate and repeated twice. Using an Olympus IX81 inverted microscope, five images per well were taken at ×100 magnification.

The number of nodes (defined as at least three cells that formed a single point) per image was quantified. To account for cell clumping, the highest and lowest values were removed from each group.

Promoter analysis and chromatin immunoprecipitation (ChIP) assay

RF24 cells were cultured in low-serum medium (0.5% serum) for 18 h and then treated with either EGFL6 (50 ng/mL) for 6 h. After treatment, ChIP assays were performed by using EZ ChIP™ kit (Millipore, Temecula, CA) as described by the manufacturer. Briefly, cross-linked cells were collected, lysed, sonicated, and subsequently subjected to immunoprecipitation with TWIST1 (Abcam, Cambridge, UK) antibody or IgG control. Immunocomplexes were collected with protein G agarose beads and eluted. Cross-links were reversed by incubating at 65°C. DNA was then extracted and purified for subsequent PCR amplification using gene-specific primers (Supplementary Table 2).

Generation of EGFL6 monoclonal antibody

Anti-EGFL6 monoclonal antibodies were identified by screening a large panel of single memory B cells collected from rabbits after immunization with recombinantly expressed human EGFL6 protein (SinoBiological, Beijing, China). Two lead anti-EGFL6 monoclonal antibodies (#93 and #135) were recombinantly expressed in HEK293 cells (Invitrogen) and purified by use of a protein A resin as we reported previously (Huang et al., 2015, Fan et al., 2015). The purified monoclonal antibodies were used for this study.

Determination of antigen binding affinity

Binding affinity of the EGFL6 monoclonal antibodies was determined by using the label-free BioLayer Interferometry (BLI) technology (ForteBio, Menlo Park, CA). Briefly, specific biosensors were used to capture the antibody on the sensor, and then the analyte (EGFL6 in a series of concentrations ranging from 55.56 to 0.69 nM) was used to bind to the antibody captured on the biosensor. The binding signal (thickness, nm) was monitored continuously to determine the kinetic constants (k_a: association rate, k_d: disassociation rate, and K_D (k_{off}/k_{on}): binding affinity) using a 1:1 fitting model with software provided by the manufacturer of the Octet instrument (ForteBio).

Wound healing assay

For the *in vivo* assays, on day 0, SKOV3ip1 cancer cells were injected into nude mice, and on day 1, mice were anesthetized with an intraperitoneal injection of ketamine (100mg/kg). Backs were sterilized with iodine and an excisional wound was made on the mid dorsal skin with a sterile scissor and animals were separated into individual cages.

Mice were divided into two groups (n=10 each). For the treatment of Control siRNA-CH and m*EGFL6* siRNA-CH, siRNA treatment was started on day 2 and given twice a week (150 μg/kg), and for antibody treatment, control IgG and EGFL6 antibody were given once weekly (5 mg/kg). The wound was measured every second day (until wound healing was completed). The tumors were harvested when the animals in any group became moribund.

Hind-limb ischemia

Critical hind-limb ischemia was induced in female nude mice after they were anesthetized with ketamine (100 mg/kg) by intraperitoneal injection. The femoral artery was ligated at its proximal origin as a branch of the external iliac artery to the distal point where it bifurcates into the saphenous and popliteal arteries. After arterial ligation, the mice were immediately assigned to the following experimental groups (n = 5): control group, ischemia-24 h, and ischemia-96 h. Color Doppler imaging (VisualSonics FUJIFILM, Toronto, Canada) was performed in three dimensions to monitor blood flow of hind limbs before and after femoral artery ligation (after 24 h and 96 h) (Krishna et al., 2016). The digital Doppler images were analyzed to assess vascular density in a region from the knee to the toe by calculating the percentage of voxels with Doppler signal above a set threshold indicating blood flow. At each time point, tissue from the ischemic limb was harvested and frozen in OCT medium. Mouse monoclonal CD31 antibody was used to determine the MVD, and mouse polyclonal EGFL6 antibody was used to determine EGFL6 expression on frozen embedded tissues according to a standard immunostaining procedure (Lu et al., 2010).

Tie2-cre;EGFL6 knockout mice generation

EGFL6$^{flox/+}$ mice were generated at ingenious Targeting Laboratory (Stony Brook, NY). To selectively delete *EGFL6* in endothelial cells, *Tie2-cre* transgenic mice (males; purchased from Genetically Engineered Mouse Facility at MD Anderson Cancer Center) were crossed to *EGFL6* floxed mice (females) to generate *Tie2-cre;EGFL6* (males). The *Tie2-cre;EGFL6* males were further crossed with *EGFL6* floxed females to obtain the *EGFL6* conditional knock-out mice. The *Tie2-cre* transgene is known for uniform expression of the cre-recombinase in endothelial cells during embryogenesis (Li et al., 2013). Genomic DNA was isolated from tail biopsies of the mouse. *Tie2-cre* transgene and floxed *EGFL6* allele were distinguished by PCR using primers (Supplementary Table 2).

Supplementary Material

Refer to Web version on PubMed Central for supplementary material.

Acknowledgments

Portions of this work were supported by the NIH (CA016672, CA109298, P50 CA217685, P50 CA098258, UH3 TR000943, R35 CA209904), the Ovarian Cancer Research Fund, Inc. (Program Project Development Grant), CPRIT (RP150551), the American Cancer Society Research Professor Award, the Blanton-Davis Ovarian Cancer Research Program, the RGK Foundation, and the Frank McGraw Memorial Chair in Cancer Research. K.N is supported by KRIBB research initiative program. S.P is supported by the Liz Tilberis Early Career Award. The GEO accession number is GSE105437.

References

BAI S, INGRAM P, CHEN YC, DENG N, PEARSON A, NIKNAFS Y, O'HAYER P, WANG Y, ZHANG ZY, BOSCOLO E, BISCHOFF J, YOON E, BUCKANOVICH RJ. EGFL6 Regulates the Asymmetric Division, Maintenance, and Metastasis of ALDH+ Ovarian Cancer Cells. Cancer Res. 2016; 76:6396–6409. [PubMed: 27803106]

BERGERS G, BENJAMIN LE. Tumorigenesis and the angiogenic switch. Nat Rev Cancer. 2003; 3:401–10. [PubMed: 12778130]

BREIER G. Angiogenesis in embryonic development–a review. Placenta. 2000; 21(Suppl A):S11–5. [PubMed: 10831116]

BUCHNER G, ORFANELLI U, QUADERI N, BASSI MT, ANDOLFI G, BALLABIO A, FRANCO B. Identification of a new EGF-repeat-containing gene from human Xp22: a candidate for developmental disorders. Genomics. 2000; 65:16–23. [PubMed: 10777661]

BUCKANOVICH RJ, SASAROLI D, O'BRIEN-JENKINS A, BOTBYL J, HAMMOND R, KATSAROS D, SANDALTZOPOULOS R, LIOTTA LA, GIMOTTY PA, COUKOS G. Tumor vascular proteins as biomarkers in ovarian cancer. J Clin Oncol. 2007; 25:852–61. [PubMed: 17327606]

CARMELIET P, JAIN RK. Angiogenesis in cancer and other diseases. Nature. 2000; 407:249–57. [PubMed: 11001068]

CHIM SM, QIN A, TICKNER J, PAVLOS N, DAVEY T, WANG H, GUO Y, ZHENG MH, XU J. EGFL6 promotes endothelial cell migration and angiogenesis through the activation of extracellular signal-regulated kinase. J Biol Chem. 2011; 286:22035–46. [PubMed: 21531721]

CHUANG CY, CHEN MK, HSIEH MJ, YEH CM, LIN CW, YANG WE, YANG SF, CHOU YE. High Level of Plasma EGFL6 Is Associated with Clinicopathological Characteristics in Patients with Oral Squamous Cell Carcinoma. Int J Med Sci. 2017; 14:419–424. [PubMed: 28539817]

DONNINGER H, BONOME T, RADONOVICH M, PISE-MASISON CA, BRADY J, SHIH JH, BARRETT JC, BIRRER MJ. Whole genome expression profiling of advance stage papillary serous ovarian cancer reveals activated pathways. Oncogene. 2004; 23:8065–77. [PubMed: 15361855]

EMING SA, BRACHVOGEL B, ODORISIO T, KOCH M. Regulation of angiogenesis: wound healing as a model. Prog Histochem Cytochem. 2007; 42:115–70. [PubMed: 17980716]

FAN X, BREZSKI RJ, DENG H, DHUPKAR PM, SHI Y, GONZALEZ A, ZHANG S, RYCYZYN M, STROHL WR, JORDAN RE, ZHANG N, AN Z. A novel therapeutic strategy to rescue the immune effector function of proteolytically inactivated cancer therapeutic antibodies. Mol Cancer Ther. 2015; 14:681–91. [PubMed: 25552368]

FERRARA N, KERBEL RS. Angiogenesis as a therapeutic target. Nature. 2005; 438:967–74. [PubMed: 16355214]

GRESSETT SM, SHAH SR. Intricacies of bevacizumab-induced toxicities and their management. Ann Pharmacother. 2009; 43:490–501. [PubMed: 19261963]

HAEMMERLE M, TAYLOR ML, GUTSCHNER T, PRADEEP S, CHO MS, SHENG J, LYONS YM, NAGARAJA AS, DOOD RL, WEN Y, MANGALA LS, HANSEN JM, RUPAIMOOLE R, GHARPURE KM, RODRIGUEZ-AGUAYO C, YIM SY, LEE JS IV, AN C, HU W, LOPEZ-BERESTEIN G, WONG ST, KARLAN BY, LEVINE DA, LIU J, AFSHAR-KHARGHAN V, SOOD AK. Platelets reduce anoikis and promote metastasis by activating YAP1 signaling. Nat Commun. 2017; 8:310. [PubMed: 28827520]

HUANG Z, CHOI BK, MUJOO K, FAN X, FA M, MUKHERJEE S, OWITI N, ZHANG N, AN Z. The E3 ubiquitin ligase NEDD4 negatively regulates HER3/ErbB3 level and signaling. Oncogene. 2015; 34:1105–15. [PubMed: 24662824]

KOSKAS M, CHEREAU E, BALLESTER M, SELLE F, ROUZIER R, DARAI E. Wound complications after bevacizumab treatment in patients operated on for ovarian cancer. Anticancer Res. 2010; 30:4743–7. [PubMed: 21115934]

KRISHNA SM, OMER SM, GOLLEDGE J. Evaluation of the clinical relevance and limitations of current pre-clinical models of peripheral artery disease. Clin Sci (Lond). 2016; 130:127–50. [PubMed: 26678170]

KRZESZINSKI JY, WEI W, HUYNH H, JIN Z, WANG X, CHANG TC, XIE XJ, HE L, MANGALA LS, LOPEZ-BERESTEIN G, SOOD AK, MENDELL JT, WAN Y. miR-34a blocks osteoporosis and bone metastasis by inhibiting osteoclastogenesis and Tgif2. Nature. 2014; 512:431–5. [PubMed: 25043055]

LANDEN CN JR, CHAVEZ-REYES A, BUCANA C, SCHMANDT R, DEAVERS MT, LOPEZ-BERESTEIN G, SOOD AK. Therapeutic EphA2 gene targeting in vivo using neutral liposomal small interfering RNA delivery. Cancer Res. 2005; 65:6910–8. [PubMed: 16061675]

LANGLEY RR, RAMIREZ KM, TSAN RZ, VAN ARSDALL M, NILSSON MB, FIDLER IJ. Tissue-specific microvascular endothelial cell lines from H-2K(b)-tsA58 mice for studies of angiogenesis and metastasis. Cancer Research. 2003; 63:2971–2976. [PubMed: 12782605]

LI S, HAIGH K, HAIGH JJ, VASUDEVAN A. Endothelial VEGF sculpts cortical cytoarchitecture. J Neurosci. 2013; 33:14809–15. [PubMed: 24027281]

LU C, BONOME T, LI Y, KAMAT AA, HAN LY, SCHMANDT R, COLEMAN RL, GERSHENSON DM, JAFFE RB, BIRRER MJ, SOOD AK. Gene alterations identified by expression profiling in tumor-associated endothelial cells from invasive ovarian carcinoma. Cancer Res. 2007; 67:1757–68. [PubMed: 17308118]

LU C, HAN HD, MANGALA LS, ALI-FEHMI R, NEWTON CS, OZBUN L, ARMAIZ-PENA GN, HU W, STONE RL, MUNKARAH A, RAVOORI MK, SHAHZAD MM, LEE JW, MORA E, LANGLEY RR, CARROLL AR, MATSUO K, SPANNUTH WA, SCHMANDT R, JENNINGS NB, GOODMAN BW, JAFFE RB, NICK AM, KIM HS, GUVEN EO, CHEN YH, LI LY, HSU MC, COLEMAN RL, CALIN GA, DENKBAS EB, LIM JY, LEE JS, KUNDRA V, BIRRER MJ, HUNG MC, LOPEZ-BERESTEIN G, SOOD AK. Regulation of tumor angiogenesis by EZH2. Cancer Cell. 2010; 18:185–97. [PubMed: 20708159]

MASIERO M, SIMOES FC, HAN HD, SNELL C, PETERKIN T, BRIDGES E, MANGALA LS, WU SY, PRADEEP S, LI D, HAN C, DALTON H, LOPEZ-BERESTEIN G, TUYNMAN JB, MORTENSEN N, LI JL, PATIENT R, SOOD AK, BANHAM AH, HARRIS AL, BUFFA FM. A core human primary tumor angiogenesis signature identifies the endothelial orphan receptor ELTD1 as a key regulator of angiogenesis. Cancer Cell. 2013; 24:229–41. [PubMed: 23871637]

NICHOL D, STUHLMANN H. EGFL7: a unique angiogenic signaling factor in vascular development and disease. Blood. 2012; 119:1345–52. [PubMed: 22160377]

OBERAUER R, RIST W, LENTER MC, HAMILTON BS, NEUBAUER H. EGFL6 is increasingly expressed in human obesity and promotes proliferation of adipose tissue-derived stromal vascular cells. Mol Cell Biochem. 2010; 343:257–69. [PubMed: 20574786]

PENG J, RAMESH G, SUN L, DONG Z. Impaired wound healing in hypoxic renal tubular cells: roles of hypoxia-inducible factor-1 and glycogen synthase kinase 3beta/beta-catenin signaling. J Pharmacol Exp Ther. 2012; 340:176–84. [PubMed: 22010210]

PRADEEP S, HUANG J, MORA EM, NICK AM, CHO MS, WU SY, NOH K, PECOT CV, RUPAIMOOLE R, STEIN MA, BROCK S, WEN Y, XIONG C, GHARPURE K, HANSEN JM, NAGARAJA AS, PREVIS RA, VIVAS-MEJIA P, HAN HD, HU W, MANGALA LS, ZAND B, STAGG LJ, LADBURY JE, OZPOLAT B, ALPAY SN, NISHIMURA M, STONE RL, MATSUO K, ARMAIZ-PENA GN, DALTON HJ, DANES C, GOODMAN B, RODRIGUEZ-AGUAYO C, KRUGER C, SCHNEIDER A, HAGHPEYKAR S, JALADURGAM P, HUNG MC, COLEMAN RL, LIU J, LI C, URBAUER D, LOPEZ-BERESTEIN G, JACKSON DB, SOOD AK. Erythropoietin Stimulates Tumor Growth via EphB4. Cancer Cell. 2015; 28:610–622. [PubMed: 26481148]

SCHAFER M, WERNER S. Cancer as an overhealing wound: an old hypothesis revisited. Nat Rev Mol Cell Biol. 2008; 9:628–38. [PubMed: 18628784]

SCHMIDT M, PAES K, DE MAZIERE A, SMYCZEK T, YANG S, GRAY A, FRENCH D, KASMAN I, KLUMPERMAN J, RICE DS, YE W. EGFL7 regulates the collective migration of endothelial cells by restricting their spatial distribution. Development. 2007; 134:2913–23. [PubMed: 17626061]

SHORD SS, BRESSLER LR, TIERNEY LA, CUELLAR S, GEORGE A. Understanding and managing the possible adverse effects associated with bevacizumab. Am J Health Syst Pharm. 2009; 66:999–1013. [PubMed: 19451611]

TONNESEN MG, FENG X, CLARK RA. Angiogenesis in wound healing. J Investig Dermatol Symp Proc. 2000; 5:40–6.

WANG X, GONG Y, WANG D, XIE Q, ZHENG M, ZHOU Y, LI Q, YANG Z, TANG H, LI Y, HU R, CHEN X, MAO Y. Analysis of gene expression profiling in meningioma: deregulated signaling pathways associated with meningioma and EGFL6 overexpression in benign meningioma tissue and serum. PLoS One. 2012; 7:e52707. [PubMed: 23285163]

WITTE L, HICKLIN DJ, ZHU Z, PYTOWSKI B, KOTANIDES H, ROCKWELL P, BOHLEN P. Monoclonal antibodies targeting the VEGF receptor-2 (Flk1/KDR) as an anti-angiogenic therapeutic strategy. Cancer Metastasis Rev. 1998; 17:155–61. [PubMed: 9770111]

YEUNG G, MULERO JJ, BERNTSEN RP, LOEB DB, DRMANAC R, FORD JE. Cloning of a novel epidermal growth factor repeat containing gene EGFL6: expressed in tumor and fetal tissues. Genomics. 1999; 62:304–7. [PubMed: 10610727]

ZHU Z, ROCKWELL P, LU D, KOTANIDES H, PYTOWSKI B, HICKLIN DJ, BOHLEN P, WITTE L. Inhibition of vascular endothelial growth factor-induced receptor activation with anti-kinase insert domain-containing receptor single-chain antibodies from a phage display library. Cancer Res. 1998; 58:3209–14. [PubMed: 9699643]

Highlight

- High EGFL6 expression in the tumor vasculature was related to poor overall survival.
- *TWIST1* regulates *EGFL6* transcriptional activity and can promote angiogenesis.
- EGFL6 regulates PI3K/AKT signaling *via* integrin-Tie2 crosstalk.
- EGFL6-antibodies effectively block tumor angiogenesis without affecting healing wounds.

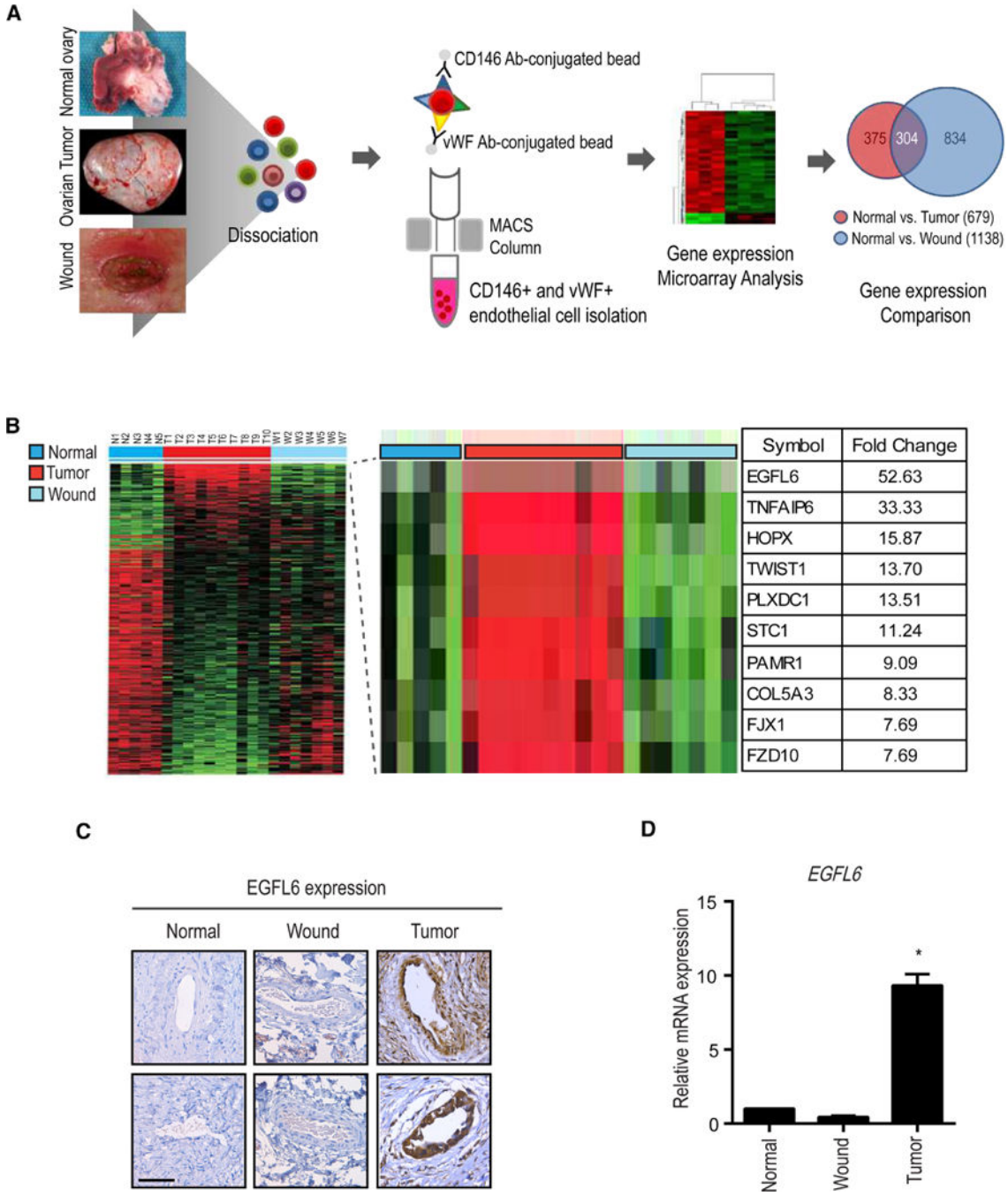

Figure 1. EGFL6 is upregulated in tumor-associated endothelial cells but not in normal ovary and healing wound tissues

a, Human normal ovary, ovarian tumor, and healing wound tissues were dissociated, and isolated endothelial cells and samples were processed for microarray. **b**, Gene microarray of endothelial cells from normal ovary, healing-wound tissue, and ovarian tumor–associated endothelial cells. **c**, Expression of EGFL6 in human normal ovary, wound, and ovarian tumor samples. Representative images were taken from different samples. Scale bar =100 μm **d**, Validation of gene microarray data using q-PCR.(Normal ovary; n = 5, Ovarian tumor;

n = 10, Wound; n = 7). Validation Error bars indicates SEM. *p<0.05 vs. Normal. See also Figure S1.

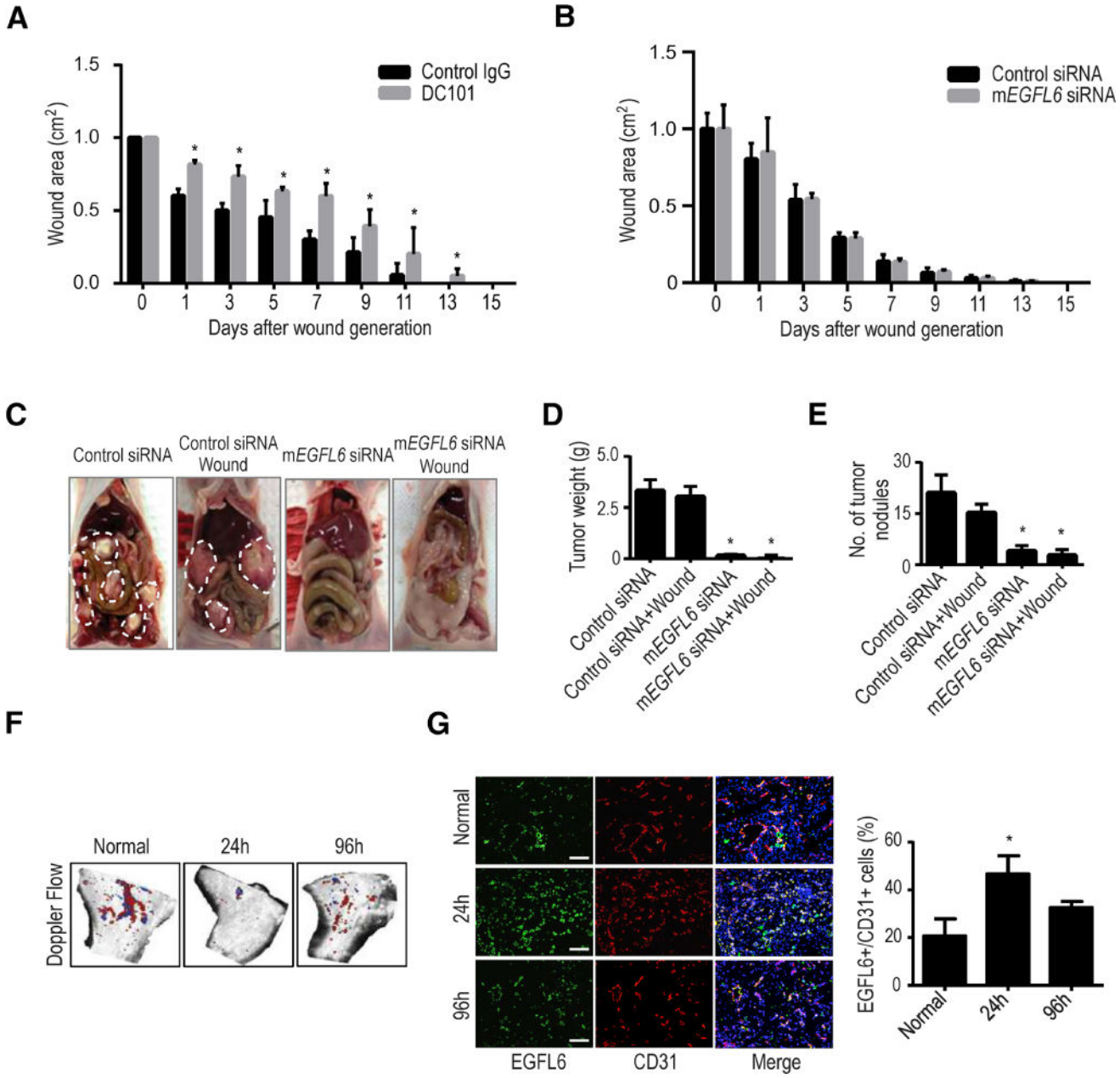

Figure 2. Effect of *EGFL6* silencing on tumor growth in orthotopic ovarian cancer mouse models

a, Graph of wound area on mice treated with either control IgG antibody or DC101 (anti-VEGFR2) quantified on days 0 through 15 after a skin excision wound. (n=10 mice per group); error bars indicate SEM. *p<0.05 vs. Control IgG. **b**, One day after SKOV3ip1 tumor cell injection, a wound was created on the dorsal side of the mice. Animals were treated with either Control siRNA-CH or m*EGFL6* siRNA-CH. Graphical depiction of wound areas quantified on days 0 through 15 after skin excision wound. **c**, Effect of m*EGFL6* silencing on tumor growth; representative images of tumor burden. Tumor weights are shown in **d** and numbers of tumor nodules in **e**. (n=10 mice per group); error bars indicate SEM. *p<0.05 vs. Control siRNA. **f**, Hind limb ischemia. After arterial ligation,

mice were separated into 3 groups (n = 5 mice per group): normal, ischemia-24 h, and 96 h. Blood flow was monitored before and after femoral artery ligation with use of serial color doppler. At each time point, tissue was harvested and frozen so that immunofluorescence staining could be performed. **g**, EGFL6 expression was increased in endothelial cells in the ischemic (hypoxic) condition compared with the normal conditions. Error bars indicate SEM. *p<0.05 vs. Normal. See also Figure S2.

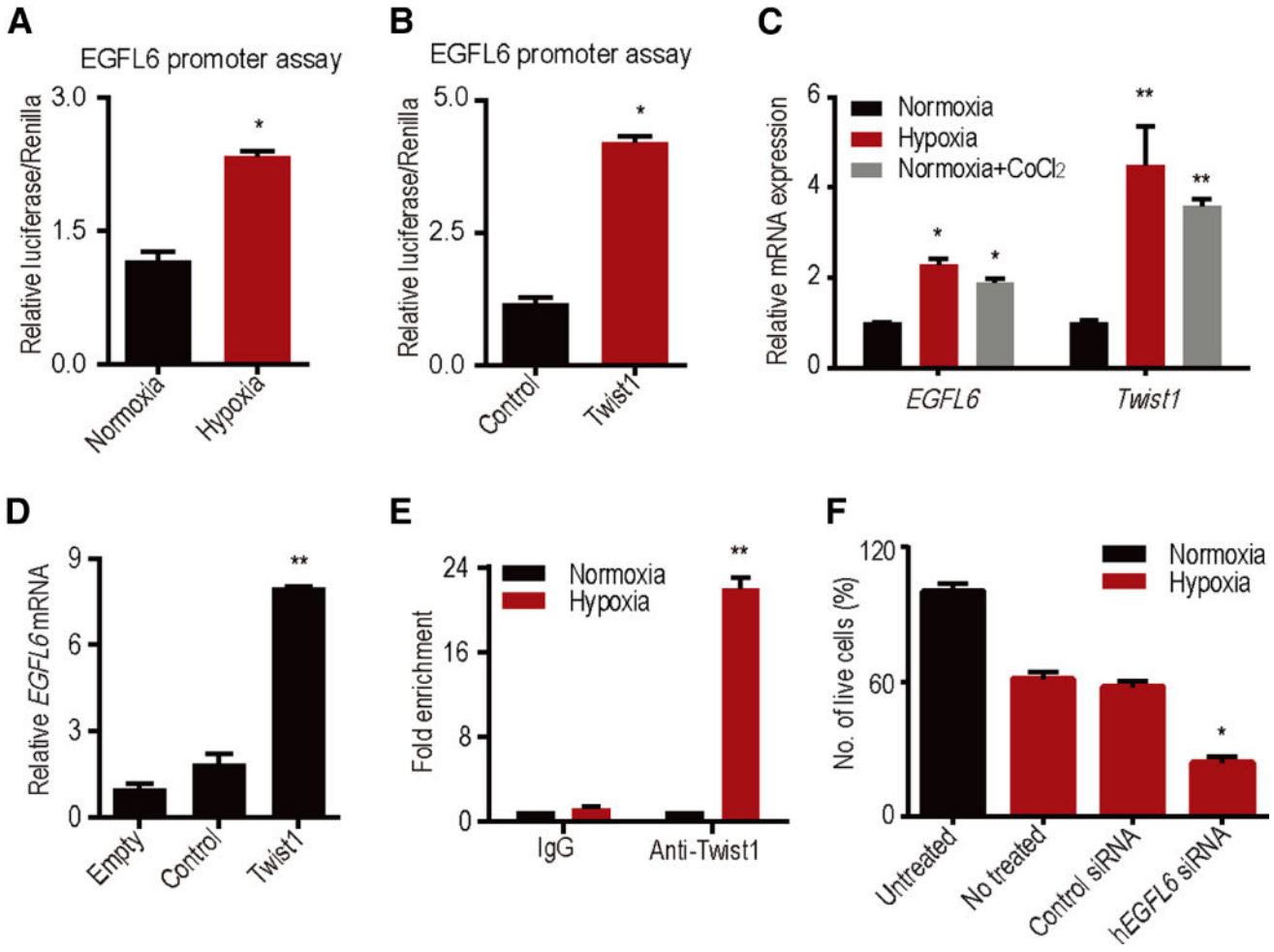

Figure 3. TWIST1 induces *EGFL6* expression under hypoxia

a, *EGFL6* promoter reporter analysis under normoxia and hypoxic conditions. **b**, *TWIST1* ectopic expression increases *EGFL6* transcription activity. **c**, Increase in *TWIST1* and *EGFL6* expression in hypoxia and $CoCl_2$ treatment. **d**, Ectopic expression of *TWIST1* increases *EGFL6* expression in RF24 cells. **e**, ChIP analysis of TWIST1 binding to *EGFL6* promoter region in hypoxia compared with normoxia. Cross-linked chromatin from RF24 cells incubated in hypoxia chamber for 48 h and immunoprecipitated with TWIST1 or IgG control antibodies. The input and immunoprecipitated DNA was subjected to PCR using primers corresponding to the base pairs upstream of *EGFL6* transcription start site. **f**, *EGFL6* gene silencing using siRNA leads to increased cell death in hypoxia condition. (n = 3) $^{**}p<0.005$, $^{*}p<0.05$ See also Figure S3.

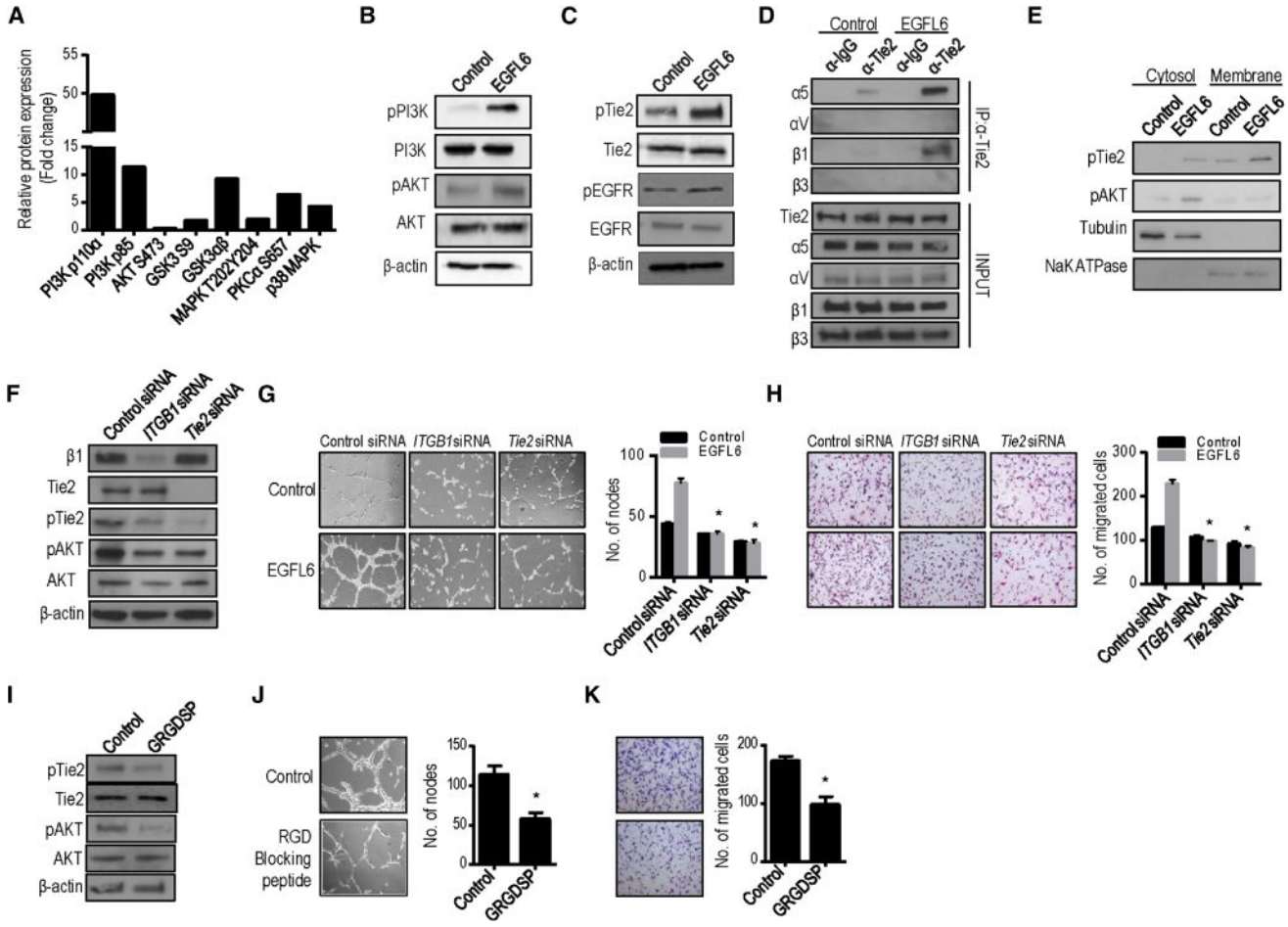

Figure 4. Treatment of EGFL6 activates PI3K/AKT signaling

a, Expression level change in selected proteins after normalization by RPPA analysis. **b** and **c**, Western blotting of EGFL6-mediated activation of PI3K/AKT signaling, Tie2 and EGFR signaling. **d**, RF24 cells treated with Control (PBS) or EGFL6. Extracts were subjected to anti-Tie2 immunoprecipitation (IP) and integrin α5, αV, β1, and β3 detected by immunoblotting. **e**, Expression level of pTie2 and pAKT in cytosol and membrane fractions with Control (PBS) and EGFL6 treatment. αβ-tubulin was used as internal control of cytosolic fraction; NaK ATPase was used as membrane marker. **f**, Silencing of *Integrin β1* (ITGB1) and *Tie2* using specific siRNAs decreases Tie2 and AKT signaling. **g–h**, Silencing of *Integrin β1* (ITGB1) and *Tie2* decreases EGFL6-mediated tube formation (**g**) and migration (**h**) in endothelial cells. **p*<0.05 vs. Control siRNA. In **i–k**, RGD blocking peptide decreases Tie2/AKT activation (**i**), tube formation (**j**) and migration (k). (n=3) **p*<0.05 vs. Control. See also Figure S4.

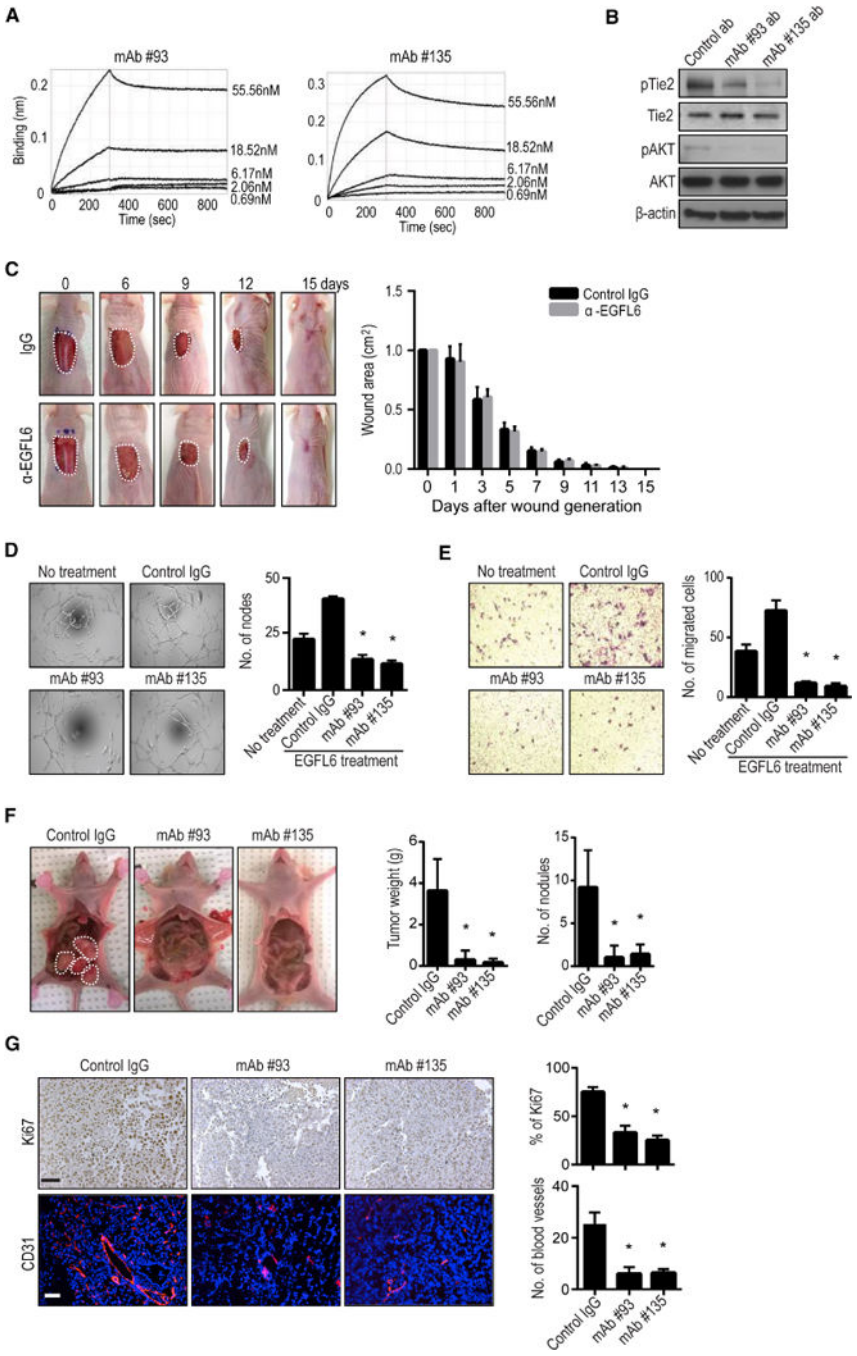

Figure 5. EGFL6 blocking antibody reduces angiogenesis and tumor growth

a, The binding affinity of recombinant EGFL6 to monoclonal antibody #93 and #135 was measured by Biacore. The dissociation constant (Kd) value of the monoclonal antibodies were calculated to be 1.89 nM (#93) and 2.19 nM (#135). **b**, Effect of EGFL6 blocking antibodies on Tie2/AKT activation in RF24 cells (n=3). **c**, Effect of EGFL6 blocking antibodies on wound healing *in vivo* (n=5 mice/group, #135; 5 mg/kg). **d** and **e**, EGFL6 antibodies decreased tube formation and migration of RF24 cells. **f**, Effect of EGFL6 blocking antibodies on tumor weight and tumor nodules in SKOV3ip1 tumor-bearing mice.

Seven days after tumor cell injection, mice were randomly divided into three groups (10 mice/group) to receive therapy: (1) Control IgG Ab, (2) EGFL6 #93, and (3) EGFL6 Ab #135 (5 mg/kg). Antibody treatment was given once a week. **g**, Effect of targeted EGFL6 on proliferation (Ki67) and microvessel density (CD31). Scale bar = 100μm. The bars in the graphs correspond sequentially to the labeled columns of images on the left. Error bars indicates SEM. *p<0.05 vs. Control IgG. See also Figure S5.

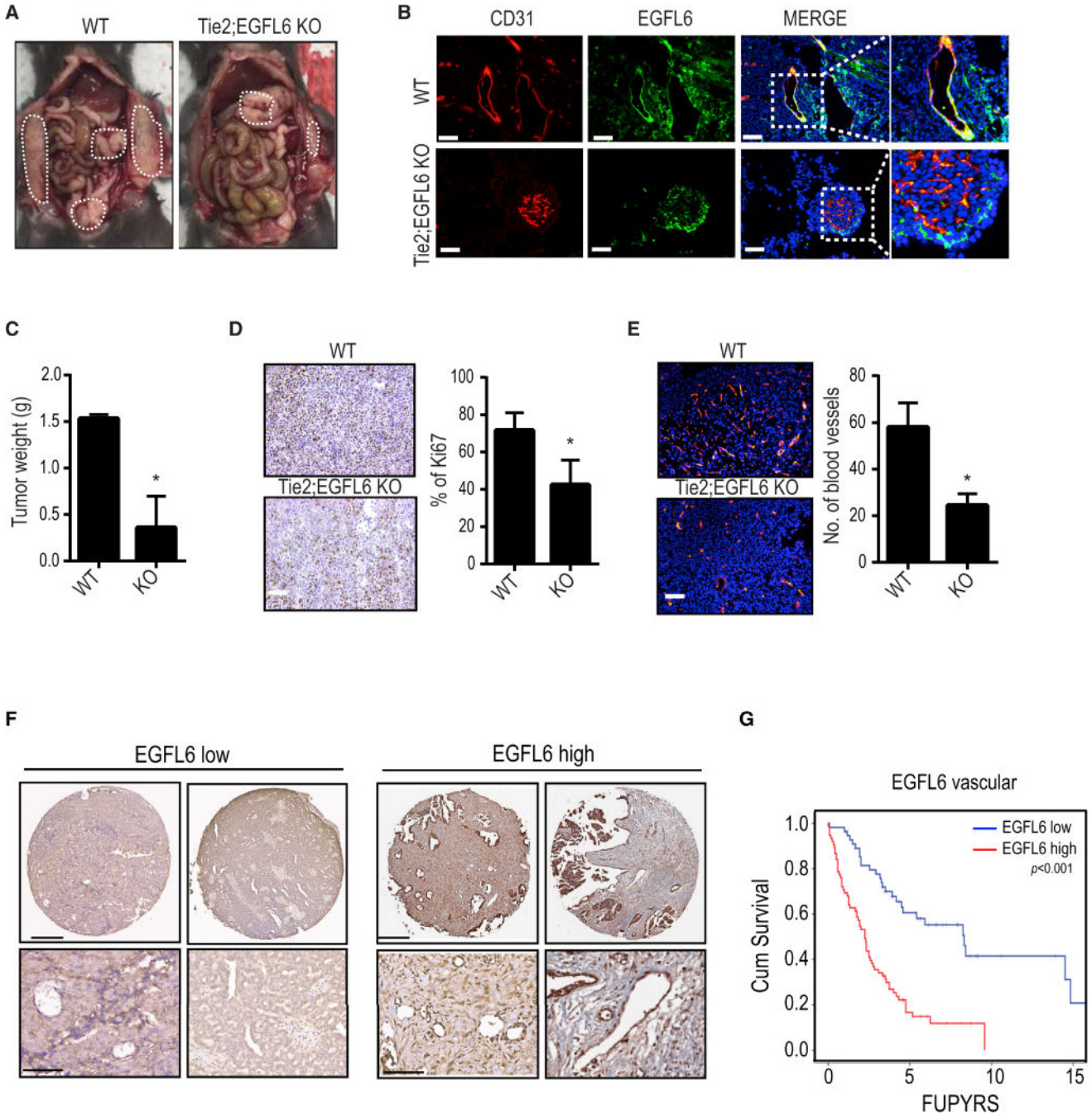

Figure 6. Effect of endothelial-specific EGFL6 knock-out on tumor growth and angiogenesis

a, Tumor growth in *Tie2;EGFL6 KO* mice (*KO*) and *WT* mice. ID8 murine ovarian cancer cells were injected into *KO* and *WT* mice (n=10 mice per group). **b**, Double immunofluorescence staining of CD31 and EGFL6 in ID8 tumor from *WT* and *KO* mice. Scale bar = 100 μm. **c**, Bar graph represents tumor weight. **d** and **e**, Proliferation (Ki67) and microvessel density (CD31) counted in *WT* and *KO* mice tumor sections. Error bars indicate SEM. Scale bar = 100 μm. **p*<0.05 vs. WT mice. **f**, Representative images of human ovarian cancer vasculature with low or high immunohistochemical staining for EGFL6. Scale bar

=200 μm. Representative images were taken from different samples. **g**, Kaplan-Meier curves of disease-specific mortality of patients whose ovarian vasculature expressed low *versus* high EGFL6. See also Figure S6 and Table S1.